RYDBERG IONIZATION: FROM FIELD TO PHOTON

G. M. LANKHUIJZEN AND L. D. NOORDAM
FOM Institute for Atomic and Molecular Physics
Kruislaan 407, 1098 SJ Amsterdam, the Netherlands
tel : 020-6081234
email : NOORDAM@AMOLF.NL
(September 27, 1996)

I. Introduction

Atoms where one of the electrons is in a highly excited state, the so-called Rydberg atoms, have proven to be a useful tool for studying the atom–radiation interaction. In the last decade a large variety of radiation sources have been used to study the ionization mechanisms of Rydberg atoms. The physical mechanism of ionization depends on the radiation frequency. For very low frequency the *field* amplitude determines the ionization, while for higher frequencies the *photon* energy is most

ISBN 0-12-003838-2

essential. In this article we will review the ionization mechanism of Rydberg atoms exposed to radiation ranging from DC fields to optical frequencies.

In the interaction of Rydberg atoms with a radiation field the Rydberg electron can gain enough energy to escape from the ionic potential: The atom ionizes. Important parameters to be considered in the ionization process are: (1) the ratio between the radiation frequency, ω, and the binding energy of the Rydberg electron, E_n; (2) the ratio between ω and the energy spacing between the Rydberg levels, ΔE_n; and (3) the coupling interaction between the Rydberg states. By studying the interaction with Rydberg atoms of different principal quantum number n at a given radiation frequency, these ratios vary. Hence to some extent frequency and principle quantum number are interchangeable (see Fig. 1). We consider the ionization of Rydberg atoms in the range of $10 < n < 100$. In this section we introduce some properties of Rydberg atoms, and highlight some of the ionization mechanisms when these Rydberg atoms are exposed to various kinds of radiation. In subsequent sections we discuss in more detail the mechanism of Rydberg atom ionization in the different radiation frequency regimes.

A. Properties of Rydberg Atoms

For an extensive overview of Rydberg atoms we refer to the excellent book by T. F. Gallagher (1994). The binding energy of the Rydberg electron in the potential of a singly charged ion is given by

$$E_{n,l} = -\frac{1}{2(n - \delta_l)^2}, \tag{1}$$

where n is the principal quantum number, and δ_l the quantum defect of the angular momentum state l (atomic units are used unless stated otherwise). This correction term (δ_l) on the binding energy arises from the presence of the core elec-

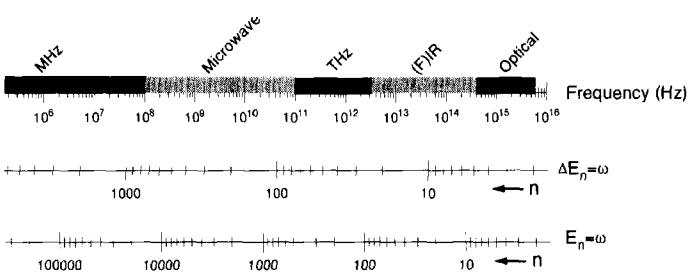

FIG. 1. The frequency range that will be discussed in this chapter is plotted in the top of the figure. The lower two bars show the principal quantum number n for which the energy spacing between n states ($\Delta E_n = 1/n^3$) and the binding energy ($\Delta E_n = -1/2n^2$) coincides with the corresponding photon energy of the radiation.

trons. The low angular momentum states will penetrate the $(Z-1)$ core electrons giving rise to a higher effective potential. This results in a more deeply bound energy for the low angular momentum states. For instance, the s-state of rubidium has a quantum defect of $\delta_0 = 3.1$.

Theoretically, the hydrogen atom is the easiest to tackle, due to the lack of core electrons and, as a result, a lack of coupling between the Rydberg states. In the experimental study of Rydberg atoms hydrogen has also been used in various experiments. However, alkali metal atoms, which can be considered one-electron atoms, are preferred experimentally because the production of a dilute gas of these atoms is rather simple. State selective production of Rydberg atoms has become possible with the invention of tunable dye lasers. The Rydberg series of the alkali atoms lies in the operation range of the tunable dye lasers. Furthermore, interesting physics arises from the existence of the core electrons, which introduce coupling between the Rydberg states. As we will see, this coupling can play a crucial role in the ionization mechanism of the Rydberg atom, especially for the cases of pulsed electric fields and microwave fields. The energy spacing of adjacent Rydberg states in hydrogen is given by

$$\Delta E_n = E_n - E_{n+1} \approx \frac{1}{n^3}. \tag{2}$$

This energy spacing is an important property when resonant transitions between Rydberg states become possible and when the frequency and intensity of the radiation field induce energy shifts of this order. The frequency of the radiation for these transitions to occur lies in the far-infrared regime.

B. Rydberg Ionization: From Field to Photon

We will now briefly mention some highlights in the ionization mechanisms organized in terms of the radiation frequency, covering the range where $\omega \ll E_n, \Delta E$ till $\omega \gg E_n, \Delta E$. The mechanisms will be discussed in more detail in the subsequent paragraphs.

1. DC-Field Ionization

When an atom is placed in a static electric field, the atomic potential is altered by the presence of the field (see Fig. 2). The tilting of the potential gives rise to a lower ionization threshold. Rydberg states with energy below the threshold can only ionize by tunnelling. We will see that the states that lie above the saddle point energy still have a finite lifetime. This is demonstrated by experiments that use short optical pulses to excite wavepackets above the saddle point energy. The evolution of the short-lived electron can be probed in two ways, either near the

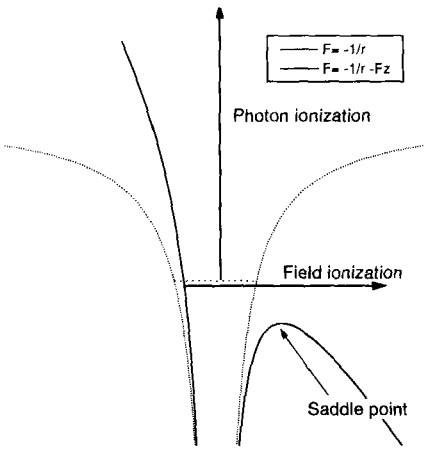

FIG. 2. The Coulomb potential experienced by a Rydberg electron without (full curve) and with (dotted curve) an external electric field applied. For DC field ionization the potential is lowered on one side, enabling electrons with energies exceeding the saddle point energy to escape from the parent ion. For optical ionization photons are absorbed by the electron leading to ionization.

core by an optical probe or near the saddle point by an atomic streak camera. It is found that the lifetime as measured by an optical technique is not the same as the time it takes the electron to leave the atom, as measured by the atomic streak camera.

2. *Ramped Field Ionization*

The ionization mechanism of a Rydberg atom exposed to ramped electric field pulses in the MHz–GHz regime (rise time of the pulses ranging from microseconds to nanoseconds) is already different from the case of DC-field ionization. During the ramp of the electric field the energy of the Rydberg state will change. The change of energy depends strongly on the coupling between the Stark states, giving rise to several ionization threshold fields. Furthermore the lifetime of the "quasi continuum" states that lie above the saddle point energy plays an important role in the ionization dynamics when half-cycle pulses are used. When the lifetime of the continuum state is shorter than the pulse duration, the ionization will be suppressed.

3. *Microwave Ionization*

Further increasing the radiation frequency brings us into the regime of microwave radiation (GHz). For the case where the GHz frequencies are smaller than the energy spacing between the Rydberg states, Stark states and Landau-Zener tran-

sitions are used to describe the ionization. Transitions from $n \rightarrow n + 1$ become possible due to the DC shift of the energy levels by the electric field, bring the levels close together. The amplitude of the field required for ionization is much lower than in the case of DC-field ionization. For high n states the frequency of the radiation field can become comparable to the energy spacing between the Rydberg levels, ΔE_n, giving rise to multiphoton type transitions.

4. THz Ionization

The production of THz radiation has recently stimulated a lot of experimental and theoretical work on the ionization of Rydberg atoms by THz radiation. Experiments have been performed with essentially unitary half-cycle pulses (HCP) with a pulse duration <1 ps, giving a large spectral bandwidth with a central frequency in the THz regime. Because the pulse duration is much shorter than the Kepler period of a Rydberg electron (2.5 ps for $n = 25$), the Rydberg electron is frozen on the time scale of the interaction with the HCP. The ionization is described using a model where the electron experiences a momentum kick from the HCP. The atom ionizes when the energy gained by the electron is larger than its original binding energy.

5. Far Infrared Ionization

Increasing the radiation frequency even further, the photon energy of the radiation becomes comparable to the binding energy of Rydberg electrons. Using far infrared radiation, transitions between Rydberg states where $\Delta n \gg 1$ have been studied. Starting from a Rydberg state the ionization occurs via a few resonant intermediate states and ionization is very efficient. A surprising exception is the ionization of lithium Rydberg atoms. The two-photon ionization cross-section of a lithium ns ($n \sim 17$) state is very small due to a Cooper minimum in the lithium bound-bound $ns \rightarrow n'p$ transition. Therefore, ionization only proceeds in a complicated manner. The Rydberg electron is first deexcited by one photon to the lower lying np state, and then climbs up the ladder ($nd \rightarrow n'p \rightarrow$ continuum) bypassing the $s \rightarrow p$ Cooper minimum in the bound-bound transitions.

6. Optical Ionization

In the optical regime, ionization can occur by absorbing a single photon ($\omega \gg E_n$) (see Fig. 2). Although in lowest order perturbation theory the frequency determines the ionization cross-section, we will see that the field amplitude can still play an important role at these high frequencies. Several mechanisms of stabilization of the Rydberg electron against ionization will be discussed depending on the laser intensity and laser pulse duration. Furthermore, at specific optical frequen-

cies the inner electrons can also be excited, giving rise to autoionizing mechanisms. Finally, Rydberg states can act as population traps in the multiphoton ionization process of ground-state atoms.

II. DC Field Ionization

When an atom is placed in a static electric field, the potential experienced by a Rydberg electron is given by

$$V = -\frac{1}{r} - Fz \tag{3}$$

where F is the electric field strength in the $-z$ direction (see Fig. 3). In the $+z$ direction the potential is lowered by the external electric field, giving rise to a saddle point in the potential surface at $z = 1/\sqrt{F}$ with an energy of $E_c = -2\sqrt{F}$. Classical ionization occurs when the binding energy of a Rydberg electron, given by $E_n = -1/2n^2$ exceeds this saddle point energy. The threshold field above which classical ionization occurs is then given by

$$F = \frac{1}{16n^4} \tag{4}$$

In an experiment by Littman *et al.* (1976) this classical threshold was clearly observed. Lithium atoms in a static electric field were excited using a tunable

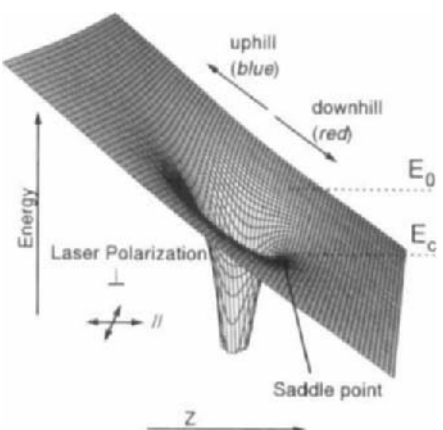

FIG. 3. Potential-energy surface of an electron in a combined Coulomb and electric field ($V = -1/r - Fz$). The classical ionization energy is lowered by the external electric field to $E_c = -2\sqrt{F}$. An electron with energy larger than E_c can escape over the saddle point.

laser. By scanning the laser frequency, the effective quantum number n^* of the excited Rydberg state was varied, showing a sharp ionization threshold when the binding energy became larger than the saddle point energy. Above E_c resonances in the ionization cross-section were observed, showing that the Rydberg states still have a non-zero lifetime. Furthermore, quantum calculations and experiments on hydrogen showed the existence of bound states above the saddle point energy (Bailey *et al.*, 1965; Koch and Mariani, 1981). From these observations it is clear that the classical description presented above is not sufficient to describe the dynamics of the electronic states in an electric field.

A. Stark States

When a hydrogen atom is placed in an electric field the degeneracy of the angular momentum states is lifted by the field. As the angular momentum (l) is no longer a conserved quantity in the field we use a new quantum number, k, which labels the parabolic Stark states in the electric field. The energy of these Stark states is given to first order by

$$E_{n,k} = -\frac{1}{2n^2} + \frac{3}{2}Fnk \tag{5}$$

where F is the electric field strength and k ranges from $-n + 1, -n + 3, .., n - 1$. From Eq. (5) we see that the energy of the Stark state is linearly depending on the electric field strength, F, showing that each k-state has a fixed electric dipole moment, independent of the electric field. States with $k > 0$ are called blue states because their energy increases as a function of the electric field, and states with $k < 0$ are called red states. The blue Stark states are located on the uphill side of the potential and the red states are on the downhill side (see Fig. 3). In the case of hydrogen there is no coupling between the Stark states. Because the blue (uphill) Stark states are located far away from the saddle point, they can only ionize via tunnelling to the continuum. The tunnelling rates of these blue states have been calculated (Bailey *et al.*, 1965) and measured (Koch and Mariani, 1981). The lifetimes can be so long ($> \mu s$) that the states are quasi stable even though their energy exceeds the saddle point energy in the potential.

For non-hydrogenic atoms the Stark states are coupled by the presence of the core electrons. The blue states can now ionize on a much faster time scale through coupling with the red continuum states. In an experiment by Littman *et al.* (1978) the ionization rate of the sodium $(n, k, m) = (13, 3, 2)$ state in the region of an avoided crossing with the rapidly ionizing red $(14, -11, 2)$ state was measured by scanning the electric field strength. A sharp increase in the ionization rate was observed (from 10^6 s^{-1} to $>10^8$ s^{-1}) at the avoided crossing between the two states, showing the effect of the coupling between the slowly ionizing and the fast ionizing state.

The lifetime of these "quasi continuum" states is also reflected in the width of the resonances as observed in an absorption spectrum. In Fig. 4 an absorption spectrum is shown of rubidium in an electric field of 4.3 kV/cm (Lankhuijzen and Noordam, 1995b). The complex structure of observed resonances can be attributed to Stark states belonging to several n-manifolds. Close to E_c we observe sharp resonances, limited by the laser resolution of 0.2 cm^{-1}, indicating long-lived states. For increasing energy of the exciting laser we observe broader peaks in the spectrum, indicating lifetimes on the order of a few picoseconds. In a similar experiment by Freeman *et al.* (1978) a resonant structure above the *zero-field* ionization limit was observed in rubidium in a static field of 4.335 kV/cm. The externally applied electric field induces shape resonances above the zero-field ionization limit. These resonances have also been observed in hydrogen (Glab and Nayfeh, 1985a, 1985b; Rottke and Welge, 1986) and are more pronounced due to the lack of couping with the red continuum states.

B. Wavepacket Decay in an Electric Field

The ionization dynamics of Stark states above the saddle point have been studied using short optical pulses to excite a coherent superposition of the "quasi continuum" states. Using optical techniques the decay of the wavepacket is monitored by measuring the amount of wave function returning to the core region as a func-

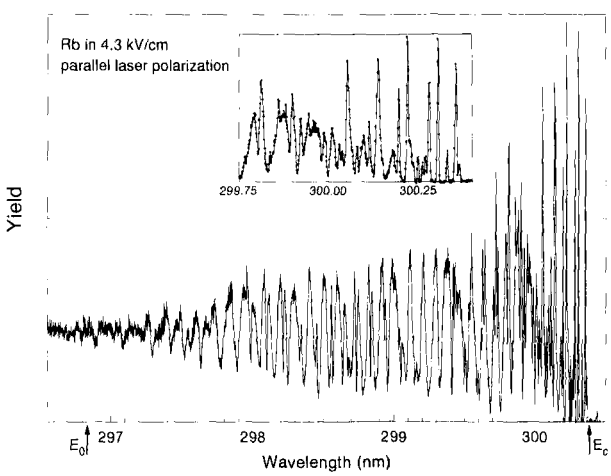

Fig. 4. Ionization yield of rubidium in an electric field of 4.3 kV/cm as a function of the wavelength. The laser polarization was chosen parallel to the electric field. The upper graph shows a magnified view of the spectrum from 299.5–300.5 nm (from Lankhuijzen and Noordam, 1995b).

tion of time. In an experiment by Broers *et al.* (1993, 1994; Christian *et al.*, 1993) a technique called Ramsey interferometry (Noordam *et al.*, 1992a) was used to measure the wavepacket decay of rubidium atoms in a static electric field. In these experiments a picosecond optical pulse excites a wavepacket above the saddle point energy. After a delay, τ_d, a second identical pulse is applied to probe the amount of wave function that has returned to the core region. In this way the evolution of the wavepacket can be observed.

Equivalently, in the frequency domain the absorption spectrum of rubidium in an electric field has been measured. It was shown (Lankhuijzen and Noordam, 1995b) that by Fourier transforming the relevant part of the frequency domain spectrum, the recurrence spectrum as measured with the Ramsey technique is obtained. A disadvantage of using optical techniques to study the *ionization* dynamics is the fact that the dynamics of the Rydberg electron can only be probed near the core. In the study of the ionization dynamics of atoms one would prefer to measure time resolved at the *escape* of the electron from the ionic potential, as this defines the ionization event.

Using an atomic streak camera (Lankhuijzen and Noordam, 1996a), the escape of the electron has been measured directly in the time domain (Lankhuijzen and Noordam, 1996b). The atomic streak camera measures the escaping electron flux from the atom with picosecond time resolution. In the experiment, rubidium atoms were excited in a static electric field of 2.0 kV/cm by a short optical pulse. The excitation energy was chosen to be above the saddle point energy, thus creating an autoionizing wavepacket. By measuring the time-dependent electron flux with an atomic streak camera the ionization dynamics were resolved.

In Fig. 5(a) a time resolved ionization spectrum of rubidium excited with a 4 ps pulse around 0.67 E_c is shown, where E_c is the saddle point energy. Inspection of the figure shows that instead of observing an exponential decaying type of wavepacket, the main ionization was surprisingly delayed 12 ps. The polarization of the laser used to excite the wavepacket was chosen perpendicular to the electric field. The wavepacket will therefore be located perpendicular to the electric field. Because the electron can only escape in the $+z$ direction it is still bound in the direction perpendicular to this axis. The wavepacket needs to reorient itself in the direction of the saddle point to escape. This reorienting can occur by scattering from the core electrons. The scattering in turn depends on the average value of the angular momentum of the wavepacket. For this particular case, the excited wavepacket makes an oscillation in angular momentum in ~ 6 ps. Excited as a low angular momentum state, the wavepacket begins to increase its angular momentum. When the wavepacket is in a high angular momentum state it will be located far away from the core electrons ($r_{mm}(l) \propto l(l+1)$), making it impossible to scatter. From Fig. 5(a) we observe that the wavepacket ionizes dominantly at the second angular recurrence. In Fig. 5(b) the corresponding recurrence spec-

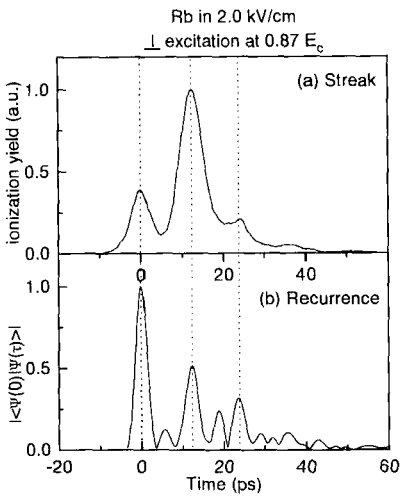

FIG. 5. Comparison between time-resolved ionization spectrum as measured by the atomic streak camera (a) and recurrence spectrum (b). The excitation is at an energy of 0.87 E_c. The laser polarization is perpendicular to the electric field of 2.0 kV/cm. In the upper spectrum the electron is probed at the saddle point, whereas in the lower spectrum the electron is probed near the core (from Lankhuijzen and Noordam, 1996b).

trum is plotted. This spectrum is a measure for the amount of wave function that comes back to the $l = 1$ state as a function of time. We see that due to dispersion in the wavepacket, the amplitude is rather low after the first oscillation in angular momentum at $\sim$ 6 ps. The second angular recurrence, however, gives a high amplitude indicating that a larger fraction of the wavepacket returns to low angular momentum states. This causes the scatter event with the core electrons leading to the large ionization at 12 ps observed in Fig. 5(a). These spectra have been reproduced by a Multilevel Quantum Defect Theory (MQDT) calculation by Robicheaux and Shaw (1996). In their calculation they could observe the scatter event by observing the transfer of population from a closed channel (bound states) into an open channel (ionizing states) when the wave function returned to the core region.

From the comparison of the recurrence spectra with the streak spectra the conclusion can be drawn that the lifetime as measured by an optical technique is not the same as the time it takes the electron to leave the atom. This conclusion can be drawn by probing the Rydberg electrons at different locations in the potential well. The Rydberg electron can be far away from the core, invisible for optical techniques, but still be captured in the attractive force of the parent ion. When the electron does not pass the core before ionizing, the electron appears to be ionized for an optical technique, but in fact has not yet escaped from the atom.

III. Ramped Field Ionization

A. Ionization by Ramped Electric Fields

In the previous section we saw that an externally applied electric field will lower the ionization threshold of a Rydberg atom. We will now discuss the case where the electric field is not stationary, but has a pulsed character.

How Rydberg states evolve from zero-field angular momentum states to Stark states that reach the ionization threshold can be best understood in terms of a Stark energy level diagram (see Fig. 6). In this figure the energy levels of rubidium are plotted as a function of the external electric field. Inspection of the figure shows a few important features: First, every n has its own manifold of states, composed of the so-called parabolic k-states. The upper states within a manifold, blue states, increase their energy as a function of the applied electric field and are located uphill in the potential (see Fig. 3), while the red states decrease their energy and are located on the downfield side. Second, the low angular momentum states have a different zero-field energy than the high angular momentum manifold states due to their quantum defect (see Eq. 1). Third, the Stark states exhibit avoided crossings due to the coupling between the states.

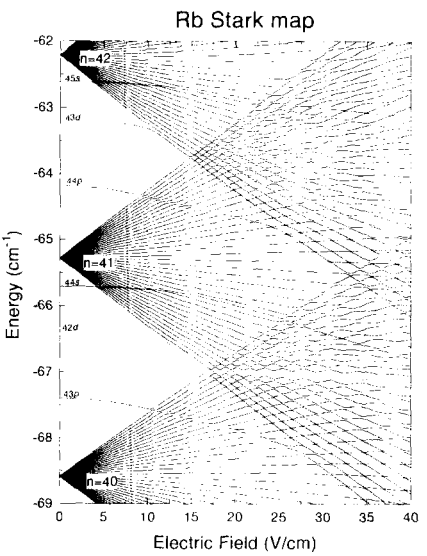

FIG. 6. Energy levels of rubidium around $n = 41$ as a function of the static electric field. The low angular momentum states ($l \leq 2$) have a different zero-field energy than the higher angular momentum states due to their quantum defect. The dotted trajectory shows the adiabatic field ionization path of the $42d$ state.

When the electric field is ramped, these avoided crossings, also called Landau-Zener crossings, can be traversed in two different ways depending on the speed at which the crossing is taken (see Fig. 7). How the crossings are traversed determines at what field strength the atom will ionize. The probability of making a diabatic transition is well approximated by the Landau-Zener transition probability (Landau and Lifshitz, 1977),

$$P_{\text{diabatic}} = \exp\left(-\frac{\pi \Delta E^2}{2 dE/dt}\right), \tag{6}$$

where ΔE is the energy splitting at the avoided crossing and dE/dt can be written as $dE/dF \times dF/dt$ where dE/dF is the field-dependent Stark shift between the two levels, and dF/dt is the slew rate of the electric field. From Eq. (6) we see that for slow field ramps (i.e., $dE/dt \ll \Delta E^2$), all the population follows the adiabatic path, whereas for fast field ramps (i.e., $dE/dt \gg \Delta E^2$), all the population follows the diabatic path (see Fig. 7). If we for instance start in the $42d$ state and slowly switch on the electric field, the population follows the dashed adiabatic trajectory of Fig. 6 and reaches the ionization threshold at the $F = 1/16n^4$. In this case the energy of the state has hardly changed (it can clearly be distinguished from the $41d$ or $43d$). When the sweep speed is increased, part of the population will follow the diabatic path at the intersection of the $n = 40$, $n = 41$ manifold and may continue to make diabatic traversals of avoided crossings further down in energy, eventually ionizing at a higher field strength of $F = 1/9n^4$. The decreasing energy of the Stark states implies that a higher field strength is needed to suppress the saddle point energy sufficiently. This adiabatic/diabatic ionization behavior has

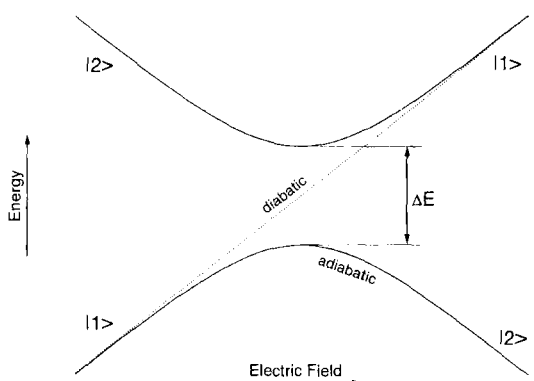

FIG. 7. A Landau-Zener crossing can be traversed in two different ways: For fast sweep rates of the field the crossing is traversed diabatically (dotted line), not changing the character of the state, whereas for slow sweep rates the crossing is traversed adiabatically (full line) changing the character of the state from $|1\rangle$ to $|2\rangle$.

been demonstrated very clearly by Neijzen and Dönszelmann (1982) (see Fig. 8). In their experiment the $66p$ Rydberg state of indium was exposed to an electric field pulse with a varying slew rate. For slow slew rates mainly adiabatic ionization occurred at the $F = 1/16n^4$ threshold ((1) in Fig. 8). When the slew rate was increased the $66p$ population makes one adiabatic crossing as it joins the adjacent n manifold. From then on it stays on the diabatic path (2) in Fig. 8, giving rise to a higher threshold field at $F = 1/9n^4$.

For even higher slew rates another interesting ionization mechanism was observed. The slew rate is now fast enough to make a diabatic crossing at the encounter of the adjacent manifold. Blue states are populated, which follow an upward path in energy as the field is ramped; path (3) in Fig. 8. Because these blue states are located on the uphill part of the potential their ionization rate only becomes fast enough when the field strength is about three times higher than the classical ionization limit. The lifetime of the "quasi continuum" states now plays an important role in the ionization. From Fig. 8 we see that for even faster slew rates (lowest graph) the ionization appearing from the third path is shifted to even higher field strength. The population survives the electric fields ranging from 20–60 V/cm because the lifetime in that range is longer than the time the population spends in that region.

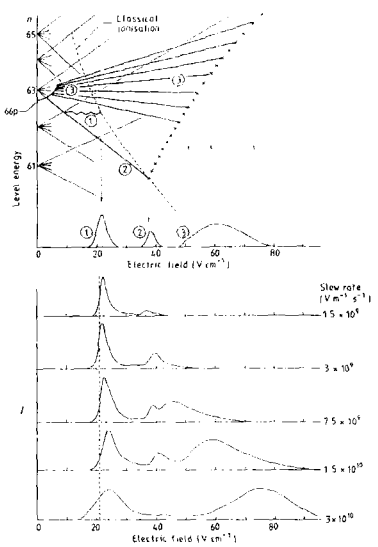

FIG. 8. The ionization signal of the $66p\ ^2P$ state as a function of the increasing electric field for various slew rates of the field pulse. The ionization signal is given in arbitrary units and the area under the curve has not been normalized. The upper part of the figure schematically explains the origin of the observed peaks (from Neijzen and Dönszelmann, 1982).

A very useful application of ramped field ionization is state-selective field ionization. This technique is widely used to determine the Rydberg population of an atom state selectively (Gallagher, 1994). The Rydberg atoms are exposed to a slowly increasing electric field, enabling the electron to follow the adiabatic path to the $F = 1/16n^4$ threshold leading to ionization. By measuring the electrons or ions as a function of time, and knowing the time characteristics of the electric field pulse, the binding energy of the Rydberg population can be retrieved, thus determining the originally populated states. The technique can also be used to determine the angular momentum distribution of the Rydberg population confined to a single manifold. The zero-field energy spacing between the angular momentum states is too small to be resolved, but the higher angular momentum states will follow a diabatic route, giving rise to a higher ionization threshold that can be resolved more easily.

B. Ionization by Half-Cycle Pulses

A natural continuation of the ramped field experiment is to switch the electric pulse off as well. By turning the electric field on and off very quickly, the Rydberg atoms are exposed to a short unidirectional electric field pulse, which brings the population into the "quasi continuum" for a short time before returning it back to zero field again. We will discuss here the interaction of these so-called half-cycle pulses with Rydberg atoms in the regime where the pulse duration is much longer than the Kepler orbit time of the Rydberg electron: $T_p \gg T_n$. For a discussion on $T_p \ll T_n$ we refer to section V.

In an experiment by Kristensen *et al.* (1997), rubidium Rydberg atoms were exposed to half-cycle pulses of different rise/fall times, duration, and amplitude. In Fig. 9 the remaining Rydberg population after exposure to two different half-cycle pulses is shown as a function of the scaled field $\tilde{F} = F/n^{*4}$. In this experiment the amplitude of the half-cycle pulse is kept constant, but the laser exciting the Rydberg population is scanned, therefore scanning the effective quantum number n^*. The $\tilde{F} = 1/16$ and $\tilde{F} = 1/9$ thresholds indicate the adiabatic and diabatic ionization thresholds respectively. For the pulse with the slowest rise time (9 ns rise time) we see that the onset of ionization occurs at the adiabatic $\tilde{F} = 1/16$ threshold. For the fast pulse (700 ps rise time, 1 ns duration) we observe a sharp threshold at the diabatic $\tilde{F} = 1/9$ threshold in agreement with the Landau-Zener model. For the fast pulse the diabatic path is followed, populating red Stark states dominantly. As soon as these states reach the ionization threshold at $\tilde{F} = 1/9$ they will ionize rapidly. For the pulse with a slow rise time, both red and blue states are populated and will reach the continuum by different paths. The fact that more blue states are also populated and reach the ionization threshold is reflected in the ionization behavior. An indication of this can be observed in Fig. 9, where beyond $\tilde{F} = 0.2$ there is more surviving population after the longer pulse than after the shorter pulse. This counterintuitive obser-

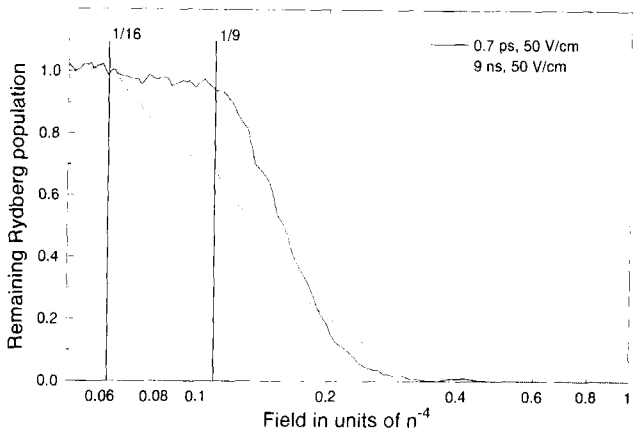

FIG. 9. Remaining Rydberg population as a function of scaled field $\tilde{F}$ after exposure to a half-cycle pulse having a 700 ps rise time (full curve) and a half-cycle pulse having a 9 ns rise time (dotted curve). Both pulses have an amplitude of 50 V/cm. The vertical lines indicate the $\tilde{F} = 1/16$ and the $\tilde{F} = 1/9$ threshold (from Kristensen *et al.*, 1997).

vation might be explained in terms of the lifetimes of the "quasi continuum" states that are populated.

In an experiment by van de Water *et al.* (1984) the surviving Rydberg population of excited triplet helium atoms, after exposure to a square half-cycle pulse, showed a remarkable non-monotonic behavior as a function of the pulse amplitude. The Rydberg atoms ($n = 19$) experienced a sharp field ramp and then a constant field for 200 ns. For ionization to occur the populated states during the constant field of the pulse need to couple with rapidly ionizing red Stark states. For certain values of the electric field the ionization was strongly reduced due to the lack of red Stark states, giving rise to the observed non-monotonic behavior in the ionization yield.

These measurements show clearly that not only the amplitude of the electric field pulse, but also the duration and slew rate are of great importance in the ionization process of the Rydberg atom.

IV. Microwave Ionization

In this section the ionization of Rydberg atoms when exposed to microwave radiation will be discussed. First we discuss the regime where the microwave radiation frequency, ω, is less then the energy spacing between the Rydberg levels, given by $\Delta E_n = 1/n^3$. The field amplitude required for ionization will be much

less than the classical field ionization limit deduced from the saddle point energy. The ionization process can be described as a sequence of half-cycle steps at the manifold crossings. Second, in experiments were high n states are populated the microwave frequency can become comparable to the energy spacing, giving rise to multi-photon type transitions leading to a different ionization mechanism. In section IV.B we will see that the frequency of the radiation starts to play a more important role in the ionization process, in particular for microwave ionization of hydrogen.

A. Regime I : $\omega < 1/n^3$

As discussed in the previous section, when a non-hydrogenic Rydberg atom is placed in a time-varying electric field, the evolution of the population can be described using Stark states and Landau-Zener transitions. This picture is also applicable to microwave ionization for $\omega < 1/n^3$ (Gallagher, 1994). In Fig. 10 the Stark energy levels in the electric field are schematically plotted. The levels are mirrored around the zero-field axis as the microwave radiation is bipolar. Also shown is the classical ionization limit given by $F = 1/16n^4$. Starting from a particular Rydberg state and applying the many-cycle microwave pulse, the popula-

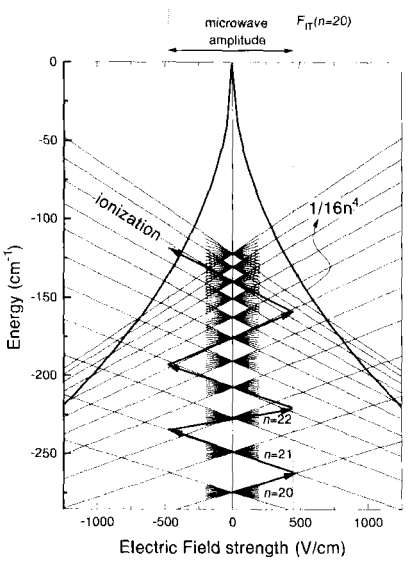

Fig. 10. Schematic graph of the Stark energy levels as a function of the electric field. For microwave amplitudes exceeding the F_{IT} value the population can follow the trajectory indicated by the arrows to the ionization limit. Note that high up in the Rydberg ladder transitions with $\Delta n > 1$ become possible.

tion will evolve through the Start states. For microwave fields below the critical value E_{IT} (see Fig. 10) the population will spread out over the $n = 20$ manifold, but is unable to reach any other manifold: Ionization will not occur. When the microwave field amplitude is high enough to reach the intersection of the adjacent $(n + 1)$ manifold, population can be transferred to the higher manifold in a single cycle of the electric field (Lankhuijzen and Noordam, 1995a). The population cannot be transferred down to the $n - 1$ manifold because the field amplitude is not large enough to reach that intersection. On subsequent cycles of the microwave field the Rydberg population can be transferred to even higher n-manifolds. If the atom interacts with the microwave radiation for a long enough time, the population will climb up the Rydberg ladder until the field reaches the classical ionization threshold at $F = 1/16n^4$: The atom ionizes. We see that the first step in the ionization process—the traversal of the first anticrossing with the adjacent manifold—is the rate limiting step for long microwave pulses. The field at which the manifolds intersect can easily be calculated and is given by

$$F_{\mathrm{IT}} = \frac{1}{3n^5}. \tag{7}$$

For $n > 6$ this so-called Inglis-Teller limit is smaller than the $F = 1/16n^4$ value. In an experiment by Pillet *et al.* (1984), sodium Rydberg atoms were ionized with long ($\sim$0.5 μs) pulses of 3.15 GHz microwave radiation. For the $|m| \leq 1$ components the onset of ionization occurred at the F_{IT} value, but for the $|m| = 2$ states the ionization occurred at the much higher field of $F = 1/9n^4$. The coupling between the $|m| = 2$ states of sodium is so small that all the avoided crossings are traversed completely diabatically, making it impossible for the population to climb the Rydberg ladder. Therefore the ionization occurred at the classical limit of the red states. This has also been studied by Mahon *et al.* (1991) as a function of the microwave frequency ranging from 10 MHz–15 GHz. In an experiment by Hettema *et al.* (1990), it was found that the ionization rate is frustrated when Stark states that lie in the middle of the manifold are excited. During the oscillations of the microwave field these middle Stark states do not change their energy, and the coupling with the reddest members of the higher manifold is frustrated.

The diabatic ionization threshold has also been observed for hydrogen (Bayfield and Koch, 1974; van Leeuwen *et al.*, 1985). If we only take into account the first order Stark effect, the slope of the Stark states, dE/dF, is constant. When a particular Stark state is put in the microwave field the Rydberg orbit does not change because the dipole moment is constant. A middle Stark state, which will remain a middle Stark state after a reverse of the field amplitude, will ionize at a much higher field then the reddest Start state of that manifold due to the lack of coupling with the red continuum states. The second order Stark effect is needed to describe the observed ionization threshold at $F = 1/9n^4$. When the second order is taken into account dE/dF is not constant any more, but is decreasing as a

function of the field. On the reversing of the microwave field each Stark state will therefore be projected onto several other Stark states. The population will be diffused through the Stark manifold and ionize once the field is large enough to ionize one of the Stark states, that is, the reddest Stark state.

From these observations we see that Landau-Zener transitions are possible whenever the frequency, ω, is in the range where a *partially* diabatic transition (see Eq. 6) is possible. The role of the frequency of the microwave radiation is rather limited, as it only determines at which of the two amplitude thresholds the ionization will occur.

In order to reach the ionization limit, many oscillations of the microwave field are needed. In an experiment by Gatzeke *et al.* (1994), short microwave pulses consisting of as little as 25 oscillations of the electric field were used to ionize Na n = 24–33 Rydberg states. Instead of the sharp thresholds observed at $F = 1/3n^5$ for the long microwave pulses, the thresholds became broader, indicating that the ionization was frustrated by the limited number of oscillations of microwave radiation field. By state selective field ionization they observed an enhanced population of higher Rydberg states after exposure to the shortest microwave pulses (25 cycles). Recently Watkins *et al.* (1996) used even shorter microwave pulses, down to only 5 oscillations of the microwave field at 8 GHz to ionize Na n = 32–44d Rydberg states (see Fig. 11). Not only did they observe a broader threshold in the ionization signal as a function of the microwave amplitude, but for the shortest pulses (6 cycles) the threshold shifted to the classical diabatic ionization limit at $F = 1/9n^4$. In this case the number of steps needed to reach the ionization threshold for a microwave ampli-

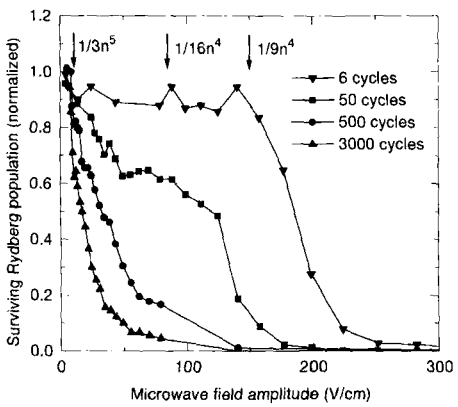

FIG. 11. Surviving Rydberg population after exposure of the 44*d* state in sodium to microwave pulses of various duration. For the longest pulse ionization occurs at the $F = 1/3n^5$ threshold. For the shortest pulse the ladder climbing is frustrated and ionization takes place at the $F = 1/9n^4$ threshold (from Watkins *et al.*, 1996).

tude corresponding to $F_{IT} = 1/3n^5$ is not sufficient. Using state selective field ionization after the short microwave pulse was applied to the $n = 24s$ state, they were able to determine that the population was trapped in higher and lower Rydberg states ($n = 23$–30) due to the limited number of cycles.

We have seen that, for microwave ionization of Rydberg atoms following the mechanism of climbing the Rydberg ladder, Landau-Zener transitions are needed to transfer the population up the Rydberg ladder. The transition should lie in the intermediate regime between a fully diabatic and adiabatic transition, putting some constraints on the frequency of the microwave radiation.

B. Regime II : $\omega \sim 1/n^3$

When the frequency of the microwave radiation becomes comparable to the zero-field Rydberg spacing, the corresponding slew rate of the field becomes so large that the Landau-Zener picture is not applicable any more and microwave ionization is described as a combination of photon transitions to higher Rydberg states followed by field ionization of this higher Rydberg state. These photon transitions have been observed in hydrogen. In an experiment by Bayfield and Koch (1974) hydrogen $n \sim 65$ (23 GHz spacing between neighboring states) atoms were exposed to microwave radiation of different frequencies. For frequencies of 30 MHz and 1.5 GHz the diabatic ionization threshold was found to occur at the field value of $F = 1/9n^4$. Because the Stark states are not coupled in hydrogen, the population transfer to higher n-manifolds was not possible, giving rise to the classical ionization limit. However, in the case of 9.9 GHz microwave radiation the required field for ionization was *lower* than this classical limit. In an experiment by van Leeuwen *et al.* (1985), the ionization of hydrogen by 9.9 GHz was studied by varying the initial Rydberg n-state. For the case where $\omega \ll 1/n^3$ the ionization occurred at the classical $F = 1/9n^4$ limit, but approaching the regime $\omega \sim 1/n^3$ the ionization threshold dropped well below this classical threshold. This was well explained by the mechanism of multiphoton transitions to higher lying n-states and subsequent ionization of that state at the $F = 1/9(n + \Delta n)^4$ threshold field.

In an experiment by Galvez *et al.* (1988) the regime from $\omega < 1/n^3$ to $\omega > 1/n^3$ was investigated for microwave ionization of hydrogen by varying the principal quantum number n (see Fig. 12). The threshold fields for ionization lie well below the classical limit ($n_0^4 F = 1/9$) in this regime and exhibit well defined structure. The observed structure is explained in terms of rational fractions of $n_0^3\omega$ at 1/1, 2/1, 5/2, etc., indicating a single-photon excitation to the $n + 1$ state, a two-photon excitation to the $n + 1$ state, and a five-photon excitation to the $n + 2$ state respectively.

There are many more states involved in the ionization process than in excitation to adjacent manifold states, making it more difficult to observe these resonances. However, in an experiment by Richards *et al.* (1989), a resonance in the

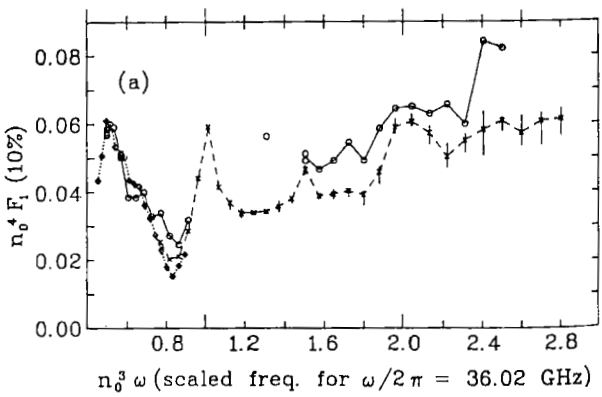

FIG. 12. Ten percent ionization threshold field for microwave ionization of hydrogen by 36.02 GHz as a function of n. Also plotted are 3D classical calculations (cross and diamond) (from Galvez *et al.*, 1988).

ionization yield was observed (see Fig. 13). In their experiment they measured the $n = 38$ ionization yield of hydrogen resulting from a microwave field of 9.92 GHz. By increasing the amplitude of the microwave radiation a non-monotonic behavior of the ionization yield was observed. At a particular field strength of the microwave field, resonant transitions occur as a result of the AC Stark shift

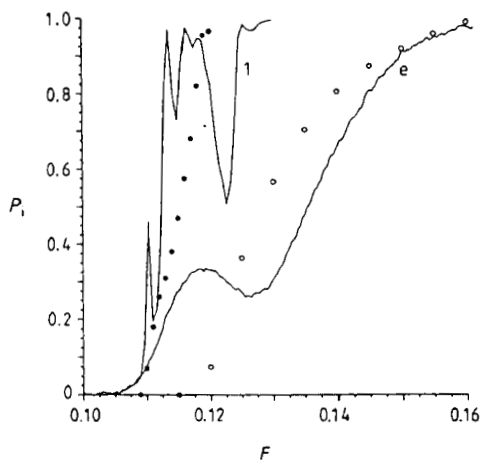

FIG. 13. Measured ionization fraction of the $n = 38$ state of hydrogen exposed to a microwave field of 9.92 GHz as a function of the microwave amplitude (curve (e)). Also plotted are a one-dimensional quantum calculation (curve (1)), one-dimensional classical calculation (full dots), three-dimensional classical calculation (open dots) (from Richards *et al.*, 1989).

induced by the microwave field shifting the states into resonance. There is no clear understanding of the states responsible for the resonance because of the large amount of states involved in the problem.

V. THz Ionization

In recent years the production of THz radiation has stimulated a lot of experimental and theoretical work on the interaction of this type of radiation with Rydberg atoms. THz radiation can be generated by illuminating a biased GaAs wafer with a femtosecond optical pulse (You *et al.*, 1993). The radiation, produced by accelerating charge carriers in the wafer, is an almost unitary half-cycle of the electromagnetic field with a temporal shape given by the envelope of the optical pulse. Because the duration of this optical pulse is ~0.5 ps, the generated radiation has frequency components well into the terahertz regime.

In an experiment by Jones and Bucksbaum (1993), the ionization threshold of sodium *nd* Rydberg atoms after exposure to such a half-cycle pulse (HCP) has been measured. From these measurements a scaling law was deduced: The amplitude, F_0, of a HCP needed to ionize a Rydberg atom scales as

$$F_0 \propto 1/n. \tag{8}$$

This scaling law, which is very different from the scaling laws presented in the former sections (see Eqs. 4, 7), was explained by Reinhold *et al.* (1993). In the regime where the radiation frequency $\omega \gg \Delta E_n$, or equivalently the pulse duration, T_p, is much less than the classical round-trip time of the electron, T_n, the ionization can be described using the impulse kick model. In this model it is assumed that the Rydberg electron does not move during the pulse, but gains momentum from the THz pulse in the form of a momentum kick given by

$$\Delta p = F_0 \int_{-\infty}^{+\infty} u(t)\mathrm{d}t, \tag{9}$$

where F_0 is the field amplitude and $u(t)$ is the normalized temporal profile of the HCP. The classical momentum of a Rydberg electron can be calculated from its binding energy $E_n = -1/2n^2$ and is given by $p_0 = \sqrt{2E_n} = 1/n$. The change in total energy of the Rydberg electron after excitation with the half-cycle pulse is then given by

$$\Delta E = (\vec{p}^{\,2} - \vec{p}_0^{\,2})/2 = \vec{p}_0 \cdot \Delta\vec{p} + \Delta\vec{p}^{\,2}/2 \tag{10}$$

where $\vec{p} = \vec{p}_0 + \Delta\vec{p}$. We see that for $\Delta p \gg p_0$ the change in energy is given by $\Delta E \simeq \Delta\vec{p}^{\,2}/2$. When the change in energy exceeds the binding energy of the Rydberg electron ($\Delta E > 1/2n^2$), the atom can ionize, giving the relation $\Delta p \propto F_0 > 1/n$. In Fig. 14 the calculated scaled fields for 10 percent ionization of hydrogen are plot-

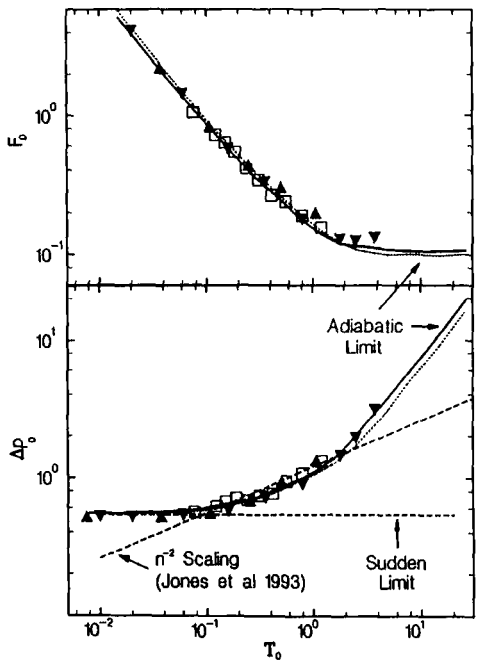

FIG. 14. Scaled field (upper figure) and scaled momentum transfer (lower figure) for 10 percent ionization threshold of $H(n, l = 2, m = 0)$ atoms as a function of the scaled pulse duration: classical results for inverse parabolic (full curve) and rectangular (dotted curve) pulses, quantum mechanical result for ionization of the $10d$ (full triangle) and $5d$ (inverted full triangle) states for rectangular pulses and experimental data by Jones and Bucksbaum (1993) for Na(nd) atoms, multiplied by a factor 2.5 (open squares) (from Reinhold *et al.*, 1993).

ted as a function of the scaled time $T_0 = T_p/T_n$ (full curve). From this figure we clearly see the transition from the short-pulse regime to the long-pulse regime. The long-pulse regime, that is, the adiabatic regime, has been discussed in section III, giving rise to the $F \propto 1/n^4$ scaling law. For the short-pulse regime significantly stronger pulses are needed to ionize the Rydberg atoms. Both classical and quantum calculations give the same result, indicating that the classical impulse-kick model is valid in the short pulse regime.

The characterization of these HCPs in amplitude and pulse shape is still rather difficult. Because the pulse is freely propagating through space, the integral of the electric field over time has to be zero, showing that the pulse can never be unipolar. The main HCP peak is followed by a long negative tail with low amplitude. The effect of this negative tail following the HCP can substantially alter the ionization probability (Tielking *et al.*, 1995). To circumvent this problem an experi-

ment was performed by Frey *et al.* (1996) where extremely high n-states were ionized by nanosecond unitary half-cycle pulses. The production of these nanosecond electrical pulses could be done in a much more controlled fashion giving a complete characterization of the pulses. In the experiment, n-states around $n \sim 388$ and $n \sim 520$ were exposed to half-cycle pulses with durations ranging from $T_p = 2$ ns to 110 ns. The corresponding classical round trip time of these n-states is $T_n \sim 9$ ns and $T_n \sim 21$ ns respectively, enabling the researchers to study the transition from the short-pulse ($T_p \ll T_n$) to the long-pulse ($T_p \gg T_n$) regime. They found perfect agreement with the theory by Reinhold *et al.* (1993).

VI. Far Infrared Ionization

In this section we discuss the radiation frequency regime where photon-transitions between Rydberg states with $\Delta n \gg 1$ can occur. The transitions to higher lying states and subsequent ionization are determined by the resonance frequency of the radiation and the dipole matrix elements between the Rydberg states.

The ionization with far infrared radiation (FIR) is examined using blackbody radiation sources (Beiting *et al.*, 1979; Gallagher and Cooke, 1979; Figger *et al.*, 1980) and CO_2 lasers (Burkhardt *et al.*, 1993). At 300 K the energy density of the blackbody radiation peaks at a wavelength of 9.6 μm. However, the stimulated absorption and emission rates of the Rydberg states depend on the photon occupation number, which drops rapidly as a function of the photon energy. In an experiment by Beiting *et al.* (1979), the redistribution of the xenon 26*f* Rydberg state to higher states was measured for various exposure times to the blackbody radiation. They found that after a 15.5 μs exposure time Rydberg states with $n > 30$ were populated. The states were detected using state-selective field ionization (see section III). The spectra showed clear peaks in the spectrum, indicating that the populated states were low angular momentum states. This showed that photon transitions ($\Delta l = \pm 1$) to the higher lying states were indeed responsible for the population redistribution. Ionization by blackbody radiation only occurs for very high n states and long exposure times and is strongly frustrated by de-excitation to lower lying states. In an experiment by Burkhardt *et al.* (1993) the ionization from the 12*s* state in sodium by irradiation with laser light coming from a CO_2 laser (a few lines around 10μm) was studied. By changing the electric field high Rydberg states that lie just below the ionization threshold shifted into resonance, giving rise to a large enhancement of the two-photon ionization yield.

A disadvantage of using blackbody radiation to ionize an atom is the fact that the bandwidth of the incoherent radiation is enormous, making it very difficult to drive transitions between two specific Rydberg states. Recently an intense far-infrared free-electron laser has become operational (Oepts *et al.*, 1995). This laser has a much narrower bandwidth ($\Delta\lambda/\lambda = 0.1\% - 10\%$) and a large tuneability

($\lambda = 6 - 100\ \mu$m), making it possible to drive photon transitions between Rydberg states where $\Delta n \gg 1$ (Hoogenraad, 1996). Multiphoton ionization is efficient because the excitation via intermediate states is resonant within the bandwidth of the FIR laser pulse. For instance, in rubidium a resonant four-photon ionization process is possible from the $14d$ state. When this state is irradiated with 46-μm radiation, the ionization process resonantly follows the $14d \rightarrow 18p \rightarrow 24s \rightarrow 60p \rightarrow \epsilon s/d$ ladder (Hoogenraad, 1996; Hoogenraad *et al.*, 1996).

A. Far Infrared Dipole Matrix Elements

In this section we will introduce some analytical results on the matrix elements between Rydberg states. The dipole matrix elements between loosely bound states of hydrogen can be approximated semiclassically with high accuracy. The following derivation has been taken from Delone *et al.* (1994) and Hoogenraad and Noordam (1996). From the correspondence principle it follows that dipole matrix element equals the Fourier component at the transition frequency ω of the classical radial coordinate $r(t)$ of the Rydberg electron along its Kepler orbit, as follows:

$$\langle n'|r|n\rangle = \frac{1}{T_n}\int_0^{Tn} r(t)\cos\,\omega t dt. \tag{11}$$

T_n is the period of the classical orbit time ($T_n = 2\pi n^3$). For transitions between near-lying states, the transition frequency can be expressed as $\omega = (n' - n)/n^3$. In the half of the orbit where the electron moves away from the core, the trajectory of an out-going $l = 0$ orbit can be written as

$$r(t) = \frac{1}{2}(6t)^{2/3} \tag{12}$$

Note that in this equation n is absent: The orbiting times of higher n states increase as n^3, while the outer turning points (the maximal value of r) scale as n^2. Substituting the half-orbit time in Eq. 12 yields the correct n dependence of the outer turning point. By substituting Eq. 12 into Eq. 11 and using the relation $T_n = 2\pi n^3$, the matrix element is given by

$$\langle n'|r|n\rangle = \frac{6^{2/3}}{2\pi n^3 \omega^{5/3}}\int_0^{\pi(n'-n)} \phi^{2/3}\cos\,\phi \mathrm{d}\phi, \tag{13}$$

where the integral takes values between 0.5 and 1 and slowly converges to $(\Gamma(2/3)/\sqrt{3}$. The two main characteristics of matrix elements between Rydberg states are present in this formula: First, the matrix elements are normalized to the density of states (n^{-3}), so that an integral over an interval of the spectrum is normalized. Second, the matrix elements depend on the transition frequency as $\omega^{-5/3}$:

Transitions between nearby-lying states are favored over high-frequency transitions. Equation 13 can be further generalized to remove the asymmetry of exchanging the initial n and final n'. Reformulating the results of Goreslavski *et al.* (1982) in terms of the binding energy of the states, $\omega_n = 1/2n^2$, and the exact transition frequency $\omega = |\omega_{n'} - \omega_n|$ yields

$$\langle n'|r|n\rangle \approx C(-2\omega_{n'})^{3/4}(-2\omega_n)^{3/4}\omega^{-5/3}. \tag{14}$$

The matrix element consists of three parts: The densities of states in the Rydberg series at states n and n', a general frequency dependence, and a prefactor $C = 0.4108$. This prefactor is only valid for $l = 0$ states. It can, however, be replaced by a frequency and angular-momentum dependent function (Hoogenraad, 1996; Berson, 1982; Goreslavskiĭ *et al.*, 1982). In doing so the C factor stays of the same order but shows a higher value for the $\Delta l = +1$ transition compared to the $\Delta l = -1$ transition, and for transitions where the energy increases, in agreement with the Bethe rule.

B. Multiphoton Ionization of Rydberg Atoms Bypassing a Cooper Minimum

The multiphoton ionization rate of a Rydberg state depends strongly on the dipole matrix elements between the intermediate states. In general, these dipole matrix elements are rather large, making the atom very susceptible to far-infrared radiation excitation, but there are exceptions. For instance, a Cooper minimum (Cooper, 1962) exists in the bound-bound $ns - n'p$ transition in lithium, giving rise to a very low excitation probability (Hoogenraad *et al.*, 1995; Hoogenraad, 1996). In Fig. 15 the relevant energy levels of lithium are plotted. The left part of the figure shows the matrix elements for the $23s$ to np transition, with the Cooper minimum occurring around the $50p$ state. When the $23s$ state was exposed to far-infrared radiation of $\lambda = 62.5$ μm (~ 160 cm^{-1}), the measured ionization yield was much higher than expected on the basis of the presence of the Cooper minimum. By scanning the frequency of the far-infrared radiation, an enhanced ionization yield was measured at the frequency corresponding to the resonant transition from the $23s$ down to the $17p$ state. If only the direct 2-photon ionization ($23s \rightarrow 50p \rightarrow$ *continuum*) was the relevant ionization mechanism, the ionization yield would be a smooth function of the frequency, because the bandwidth of the laser pulses is much larger than the Rydberg spacing around $n = 50$. The resonance indicates that another path dominates the ionization process. Within the bandwidth of the laser, resonant transitions follow the $23s \rightarrow 17p \rightarrow 22d \rightarrow 50p \rightarrow \epsilon s/d$ *continuum*, apparently the dominant pathway in the ionization process. Due to the Cooper minimum, two-photon ionization is frustrated and a higher-order process is favored, starting with stimulated emission of a FIR photon instead of absorbing photons.

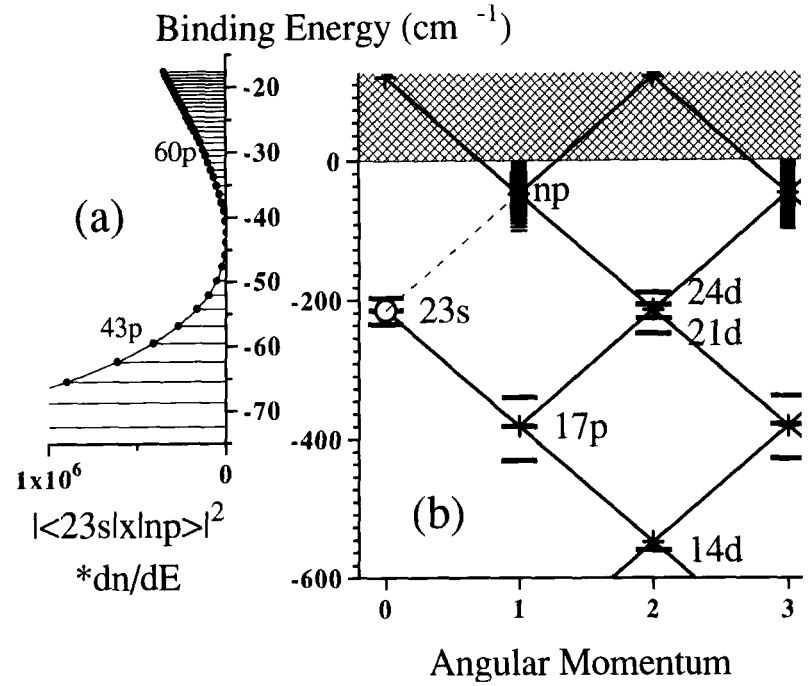

FIG. 15. (a) Squared and normalized matrix elements near the Cooper minimum in the $23s \rightarrow np$ series. The normalized matrix elements from the $23s$ to the $17p$ state are 3.8×10^9 $(a_0/Ry)^2$. (b) The frustrated direct two-photon path (starting with the dashed line) and alternative higher-order multiphoton paths to the continuum, bypassing the Cooper minimum (from Hoogenraad *et al.*, 1995).

VII. Optical Radiation

The energy of an optical photon ($0.1\ \mu m < \lambda < 1\ \mu m$) exceeds the binding energy of Rydberg states, and ionization can occur by the absorption of a single photon. Although in lowest order perturbation theory the frequency determines the ionization cross-section, the field amplitude can still play an important role at these high frequencies. It has been found that for high amplitudes of the optical radiation the ionization cross-section actually decreases (an effect known as adiabatic stabilization, which will be discussed in section VII.A). At high frequencies the excitation of inner electrons also becomes possible (section VII.B). The energy exchange of the excited inner electron with the Rydberg electron can lead to autoionization. In the final section VII.C we will see that in the process of multiphoton ionization of ground state atoms, Rydberg states can be a "dead end" en route to the ionization continuum.

Let us start with the ionization rate, R, and its physical implications. Starting from Eq. 14, it follows that the single-photon ionization rate for a low angular momentum Rydberg state ($l \ll n$) is given by (Goreslavskiĭ *et al.*, 1992).

$$R \propto n^{-3}\omega^{-10/3}I \tag{15}$$

Here we find the expected linear intensity (I) dependence. The decreasing rate with increasing photon energy (ω) reflects the decreasing overlap of the continuum wavefunction with the Rydberg state. In order to conserve momentum, photoabsorption occurs near the atomic core (Giusti-Suzor and Zoller, 1987). Hence the absorption rate is proportional to the time the electron spends near the core and is thus inversely proportional to the Kepler orbit time $T_n = 2\pi n^3$.

A. Stabilization

Several mechanisms of stabilization can prevent the Rydberg atom from completely ionizing despite the fact that the fluence of the pulse, based on Eq. 15, is sufficient for depletion. In this section we discuss three types of stabilization (for a more detailed review see Muller and Fedorov, 1996).

1. Transient Stabilization

As mentioned above, only the fraction of the extended Rydberg wavefunction near the core can absorb an optical photon. For laser pulse durations (T_p) shorter than the Kepler orbiting time (T_n), the fraction of the wavefunction that passes the core during the pulse and hence can be ionized is at most T_p/T_n. This simple picture is confirmed both by quantum calculations (Hoogenraad and Noordam, 1993) and experiment (Hoogenraad *et al.*, 1994) (see Fig. 16). This type of stabilization is called transient because more intense pulses will not ionize the atom (in contrast to Eq. 15), while longer pulses ionize the atom completely, as all the Rydberg wavefunction will pass the core during such a longer pulse. The short laser pulse drills a hole in the stationary wavefunction and as a result a nonstationary anti-wave packet is formed. The states adjacent to the initial Rydberg state are coherently populated by a Raman transition via the continuum (Yeazell and Stroud, 1991). Both frequencies required for the Raman transition are within the large bandwidth of the short laser pulse. The redistribution of Rydberg population by short laser pulses has been observed by several groups (Noordam *et al.*, 1992b; Duncan and Jones, 1996).

2. Interference Stabilization

In the case of interference stabilization (Fedorov and Movsesian, 1989) the coherent superposition of adjacent Rydberg states is not due to the short laser pulse and the resulting large bandwidth, but rather the high intensity of the laser.

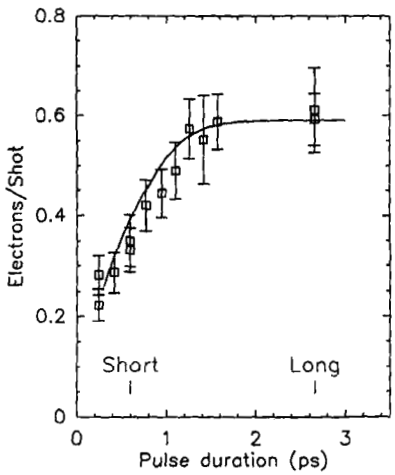

FIG. 16. The measured photoionization yield of the $6s27d^1D_2$ state in barium as a function of laser pulse duration for a constant fluence of 7.8 J/cm^2. The full curve is a calculation based on the mechanism described in the text (from Hoogenraad *et al.*, 1994).

The Rabi flopping time of the Rydberg state to the continuum becomes comparable to the Kepler orbit time (or equivalently in the frequency domain: the lifetime broadened Rydberg state overlap in energy). The transferred amplitudes out of the different Rydberg states interfere destructively in the continuum.

3. *Adiabatic Stabilization*

In the case of adiabatic stabilization the ionization is suppressed at high intensities, irrespective of the pulse duration, and adjacent Rydberg states play no role. Because the photon energy is large compared to the binding energy of the Rydberg electron, the oscillations of the optical field are rapid compared with any electronic motion. In this high-frequency limit, the electron experiences the time-averaged potential of the core plus the laser field. Calculations show that the large electron excursion due to the field (amplitude $\alpha_0 = \sqrt{I/\omega^2}$) reduces the interaction with the core and thereby the photoionization probability (Pont and Gavrila, 1990; Vos and Gavrila, 1993). Indeed, experiments show a lower ionization cross-section at higher intensities (de Boer *et al.*, 1993a; van Druten *et al.*, 1996).

B. Inner Electron Excitation and Ionization

Optical excitation of an ionic transition with the remote Rydberg electron as a spectator is known as isolated core excitation. When the Rydberg electron passes the core it can exchange energy with the excited core and autoionize. Autoion-

ization spectroscopy in which the core is excited with a narrow bandwidth low-intensity laser pulse is a field in its own right (see reviews by Sandner, 1987, and Gallagher, 1994). If the intensity of the core excitation is high enough, the Rabi frequency of the inner electron transition becomes comparable to the Kepler orbit frequency of the outer Rydberg electron. Several authors (van Druten and Muller, 1995, 1996; Robicheaux, 1993; Grobe and Haan, 1994; Hansen and Lambropoulos, 1995, 1996) have predicted that the autoionization dynamics are strongly influenced by the Rabi flopping of the inner electron. Suppose the Rydberg electron orbits as a wavepacket around the core and the inner electron is flopping with the same frequency from the ground state to the excited state. Autoionization only occurs when the Rydberg electron passes the core while the inner electron is excited. So if the core is in the ground state when the Rydberg electron passes by and the Rabi and Kepler frequency are the same, the ion will be again in the ground state at the next passage of the Rydberg wavepacket: The doubly excited state is relatively stable against autoionization. In contrast, when the Rydberg electron is in a stationary eigenstate while the pulse duration of the core excitation is short, there is a sudden turn on of the autoionization of the Rydberg atom. Once the core is excited, the incoming Rydberg electron flux penetrating the core region can autoionize. As long as fresh wavefunction penetrates the core the autoionization rate is constant. After one Kepler orbit time all the wavefunction has passed the core once and the ionization rate drops to a lower value. This stepwise decay of the autoionization as described by Wang and Cooke (1991, 1992) is very similar to the stepwise decay of a Rydberg atom when exposed to a laser field that is suddenly turned on and kept constant thereafter (Hoogenraad and Noordam, 1993). It has also been shown that off-resonant excitation of the inner electron leading to autoionization can be accomplished if the outer electron is near the core at the time of excitation. In this situation the energy mismatch of the core excitation is absorbed by the energy of the outer electron. The outer electron gives or takes energy to or from the inner electron (Story *et al.*, 1993).

As discussed above, Rydberg atoms are difficult to photoionize with pulses that are short compared to the Kepler orbit time. However, such short pulses can ionize inner electrons in a non-resonant multiphoton process. In two independent experiments (Stapelfeldt *et al.*, 1991; Jones and Bucksbaum, 1991) it was found that for a *Ba* Rydberg atom, exposed to short intense radiation, it was not the loosely bound Rydberg electron but rather the deeply bound 6s electron (10 eV) that was ionized. The Rydberg state of the neutral atom is projected on several Ba^+ Rydberg states (Vrijen, 1997; Vrijen and Noordam, 1996; Vrijen *et al.*, 1996) by suddenly kicking out the inner electron. Ionizing inner electrons while the Rydberg electron remains attached to the ionic core creates an alternative scheme for an x-ray laser (Vrijen and Noordam, 1996; Vrijen *et al.*, 1996). For instance one can start with a gas of lithium Rydberg atoms ($n = 8$). Photoionization of the inner electrons results in a hollow atom: Li^{2+} ($n = 14$). Using a second laser pulse the $n = 14$ population can be stimulated down to $n = 5$, resulting in a population inversion on the $5p \rightarrow 1s$ transition in Li^{2+} at 10.5 nm.

C. Rydberg States as Population Trap in Multiphoton Processes

Using sub-picosecond laser pulses, Freeman *et al.* (1987) demonstrated that Rydberg states play an important role in the multiphoton ionization process of ground-state atoms with optical radiation. Until recently it was believed that these intermediate Rydberg states enhance the ionization rate and no excited state population was left over after the intense pulse. Due to the large AC Stark shift (~1 eV) of the Rydberg states during the intense pulse, the states shift in and out of N-photon resonance. In fact, transfer to the subsequent Rydberg states, shifting in resonance, can deplete the ground state during the rising edge of the short pulse, (Vrijen *et al.*, 1993; Story *et al.*, 1993b). Recently de Boer *et al.* (1992, 1993b) have demonstrated that these states are indeed populated during the pulse, but that the ionization rate out of the Rydberg states (see Eq. 15) is so low that a large fraction of the population is trapped in these states. The role of Rydberg resonances in multiphoton ionization processes was recently reviewed by Vrijen *et al.* (1994).

VIII. Open Questions

Despite the vast amount of investigation on Rydberg ionization in the different frequency regimes, as summarized in this contribution, many problems are not yet solved. We will address a few problems that require further investigations, both theoretical and experimental.

The dynamics of an electron excited above the saddle point of the combined Coulomb + **static** field is particularly well studied near the core. As demonstrated by Lankhuijzen and Noordam (1996b), the behavior near the core does not disclose *when* the electron is actually ejected. As the stability of highly excited electrons in external fields is of practical relevance in plasma environments, this field deserves a more detailed study.

The mechanism of **microwave** ionization ($\omega < 1/n^3$) with long pulses is well established. However, how the quantum diffusion proceeds if the Rydberg atom is only exposed to a *few* cycles is less clear. The transfer per cycle from n to $n + 1$ is well below 100 percent and coherent addition of amplitude, transferred during subsequent cycles, will definitely play a role. Well-defined experiments investigating the coherence effects in microwave ionization are rare, and the large amount of quantum states involved requires a major computational effort. Another open question is how high in n must the electron climb before the last half cycle can ionize the atom. Half cycle ionization with (sub)nanosecond pulses suggests that the threshold field amplitude is well beyond $F = 1/9n^4$. To treat this problem theoretically, both the impulsive kick approximations, only applicable to very short pulses, and (a)diabatic sweeping up to the threshold description, fail, the latter because states above threshold are too long lived to assume direct ionization.

Ionization with half-cycle **THz** pulses is a new and exciting field with many unsolved problems. What is the influence of the core electrons (in other words, is there a difference between sodium and hydrogen)? Does the core play a role in the time of ejection of the electron from the atom? How does ionization proceed for circular states ($m = l = n - 1$), that is, is there a polarization dependence in the ionization behavior of circular states?

Single-photon ionization with **far infrared** radiation provides the electron with little excess energy. Infrared photoionization of a polarized Rydberg atom in a static field is at the unexplored border of optical ionization and a $n \rightarrow n + 1$ transition. Absorption of optical photons occurs near the core, and the rate of ionization strictly depends on the amount of initial state wavefunction near the core. For a $n \rightarrow n + 1$ transition blue/uphill n-states couple best with blue/uphill $n + 1$-states, due to their large overlap in wavefunctions. A much larger fraction of the initial state wavefunction contributes to the transition probability.

Stabilization of Rydberg atoms against photoionization with **optical** radiation, being one of the exciting new theoretical findings in the field of atoms in strong laser fields, has been verified experimentally only in a limited fashion. There is no experimental evidence of interference stabilization; adiabatic stabilization has been studied in some detail (deBoer *et al.*, 1993a; van Druten *et al.*, 1996), demonstrating that the atom is not completely ionized at high intensities. However, there is no explicit evidence for a reduced rate at very high intensities. Finally, transient stabilization has been experimentally confirmed (Hoogenraad *et al.*, 1993), but the connection with adiabatic stabilization, that is, ionization with very short and intense pulses, is unexplored, both theoretically and experimentally.

IX. Acknowledgment

The authors would like to acknowledge T. F. Gallagher and his group for the productive collaborations over many years resulting in some of the work summarized in this paper. We thank D. I. Duncan and M. J. J. Vrakking for carefully reading the manuscript. Some of the work described in this paper is part of the research program of the Stichting Fundamenteel Onderzoek van de Materie (Foundation for Fundamental Research on Matter) and was made possible by the financial support from the Nederlandse Organisatie voor Wetenschappelijk Onderzoek (Netherlands Organization for the Advancement of Research).

X. References

Bailey, D. S., Hiskes, J. R., and Riviere, A. C. (1965). *Nucl. Fusion.* 5, 41.

Bayfield, J. E., and Koch, P. M. (1974). *Phys. Rev. Lett.* 33, 258.

Beiting, E. J., Hildebrandt, G. F., Kellert, F. G., Foltz, G. W., Smith, K. A., Dunning, F. B., and Stebbings, R. F. (1979). *J. Chem. Phys.* 70, 3551.

Berson, I. Y. (1982). *Sov. Phys.-JETP.* 56, 731.
Broers, B., Christian, J. F., Hoogenraad, J. H., van der Zande, W. J., van Linden van den Heuvell, H. B., and Noordam, L. D. (1993). *Phys. Rev. Lett.* 71, 344.
Broers, B., Christian, J. F., and van Linden van den Heuvell, H. B. (1994). *Phys. Rev. A.* 49, 2498.
Burkhardt, C. E., Ciocca, M., Leventhal, J. J., Arimondo, E., Bergeman, T., and Manson, S. T. (1993). *Nucl. Instr. and Meth. B.* 56, 313.
Christian, J. F., Broers, B., Hoogenraad, J. H., van der Zande, W. J., and Noordam, L. D. (1993). *Opt. Commun.* 103, 79.
Cooper, J. W. (1962). *Phys. Rev.* 128, 681.
de Boer, M. P., and Muller, H. G. (1992). *Phys. Rev. Lett.* 68, 2747.
de Boer, M. P., Hoogenraad, J. H., Vrijen, R. B., Noordam, L. D., and Muller, H. G. (1993a). *Phys. Rev. Lett.* 71, 3263.
de Boer, M. P., Noordam, L. D., and Muller, H. G. (1993b). *Phys. Rev. A.* 47, 45.
Delone, N. B., Goreslavskii, S. P., and Krainov, V. P. (1994). *J. Phys. B: At. Mol. Opt. Phys.* 27, 4403.
Duncan, D. I., and Jones, R. R. (1996). *Phys. Rev. A.* 53, 4338.
Fedorov, M. V., and Movsesian, A. M. (1989). *J. Opt. Soc. Am. B.* 6, 928.
Figger, H., Leuchs, G., Straubinger, R., and Walther, H. (1980). *Opt. Commun.* 33, 37.
Freeman, R. R., Economou, N. P., Bjorklund, G. C., and Lu, K. T. (1978). *Phys. Rev. Lett.* 41, 1463.
Freeman, R. R., Bucksbaum, P. H., Milchberg, H., Darack, S., Schumacher, D., and Geusic, M. E. (1987). *Phys. Rev. Lett.* 59, 1092.
Frey, M. T., Dunning, F. B., Reinhold, C. O., and Burgdörfer, J. (1996). Submitted to *J. Phys. B: At. Mol. Opt. Phys.*
Gallagher, T. F., (1994). *Rydberg atoms,* 1st ed. Cambridge University Press (Cambridge).
Gallagher, T. F., and Cooke, W. E. (1979). *Appl. Phys. Lett.* 34, 369.
Galvez, E. J., Sauer, B. E., Moorman, L., Koch, P. M., and Richards, D. (1988). *Phys. Rev. Lett.* 61, 2011.
Gatzke, M., Noordam, L. D., Watkins, R. B., and Gallagher, T. F. (1994). *Phys. Rev. A.* 50, 2502.
Giusti-Suzor, A., and Zoller, P. (1987). *Phys. Rev. A.* 36, 5178.
Goreslavskii, S. P., Delone, N. B., and Krainov, V. P. (1982). *Sov. Phys.* 55, 1032.
Glab, W. L., and Nayfeh, M. H. (1985a). *Phys. Rev. A.* 31, 530.
Glab, W. L., and Nayfeh, M. H. (1985b). *Phys. Rev. A.* 31, 3677.
Grobe, R., and Haan, S. L. (1994). *J. Phys. B: At. Mol. Opt. Phys.* 27, L735.
Hanson, L. G., and Lambropoulos, P. (1995). *Phys. Rev. Lett.* 74, 5009.
Hanson, L. G., and Lambropoulos, P. in H. G. Muller and M. V. Fedorov (Eds.), *Super-Intense Laser-Atom Physics IV.* Kluwer Academic Publishers (Dordrecht/Boston/London, 1996), pp. 269–278.
Hettema, J. M., Fu, P., and Gallagher, T. F. (1990). *Phys. Rev. A.* 41, 6555.
Hoogenraad, J. H. (1986). Ph.D. thesis. University of Amsterdam (The Netherlands).
Hoogenraad, J. H., and Noordam, L. D. in B. Piraux, A. L'Huillier, and K. Rzążewski (Eds.), *Super-Intense Laser-Atom Physics.* Plenum (New York, 1993), pp. 269–278.
Hoogenraad, J. H., Vrijen, R. B., and Noordam, L. D. (1994). *Phys. Rev. A.* 50, 4133.
Hoogenraad, J. H., Vrijen, R. B., van der Meer, A. F. G., van Amersfoort, P. W., and Noordam, L. D. (1995). *Phys. Rev. Lett.* 75, 4579.
Hoogenraad, J. H., and Noordam, L. D. (1996). Submitted to *Phys. Rev. A.*
Hoogenraad, J. H., Vrijen, R. B., and Noordam, L. D. (1996). Submitted to *Phys. Rev. A.*
Jones, R. R., and Bucksbaum, P. H. (1991). *Phys. Rev. Lett.* 67, 3215.
Jones, R. R., and Bucksbaum, P. H. (1993). *Phys. Rev. Lett.* 70, 1236.
Koch, P. M., and Mariani, D. R. (1981). *Phys. Rev. Lett.* 46, 1275.
Kristensen, P., Lankhuijzen, G. M., and Noordam, L. D. (1997). *J. Phys. B: At. Mol. Opt. Phys.* 30, 1481.
Landau, L. D., and Lifshitz, E. M. (1977). *Quantum Mechanics Non-Relativistic Theory,* 3rd ed. Pergamon Press (New York).

Lankhuijzen, G. M., and Noordam, L. D. (1995a). *Phys. Rev. Lett.* 74, 355.
Lankhuijzen, G. M., and Noordam, L. D. (1995b). *Phys. Rev. A.* 52, 2016.
Lankhuijzen, G. M., and Noordam, L. D. (1996a). *Opt. Commun.* 129, 361.
Lankhuijzen, G. M., and Noordam, L. D. (1996b). *Phys. Rev. Lett.* 76, 1784.
Littman, M. G., Zimmerman, M. L., and Kleppner, D. (1976). *Phys. Rev. Lett.* 37, 486.
Littman, M. G., Kash, M. M., and Kleppner, D. (1978). *Phys. Rev. Lett.* 41, 103.
Mahon, C. R., Dexter, J. L., Pillet, P., and Gallagher, T. F. (1991). *Phys. Rev. A.* 44, 1859.
Muller, H. G., and Fedorov, M. V. (1996). *Super-Intense Laser-Atom Physics IV*, 1st ed. Kluwer Academic Publishers (Dordrecht/Boston/London).
Neijzen, J. H. M., and Dönszelmann, A. (1982). *J. Phys. B: At. Mol. Opt. Phys.* 15, L87.
Noordam, L. D., Duncan, D. I., and Gallagher, T. F. (1992a). *Phys. Rev. A.* 45, 4734.
Noordam, L. D., Stapelfeldt, H., Duncan, D. I., and Gallagher, T. F. (1992b). *Phys. Rev. Lett.* 68, 1496.
Oepts, D., van der Meer, A. F. G., and van Amersfoort, P. W. (1995). *Infrared Phys. Technol.* 36, 297.
Pillet, P., van Linden van den Heuvell, H. B., Smith, W. W., Kachru, R., Tran, N. H., and Gallagher, T. F. (1984). *Phys. Rev. A.* 30, 280.
Pont, M., and Gavrila, M. (1990). *Phys. Rev. Lett.* 65, 2362.
Reinhold, C. O., Melles, M., Shao, H., and Burgdörfer, J. (1993). *J. Phys. B: At. Mol. Opt. Phys.* 26, L659.
Richards, D., Leopold, J. G., Koch, P. M., Galvez, E. J., van Leeuwen, K. A. H., Moorman, L., Sauer, B. E., and Jensen, R. V. (1989). *J. Phys. B: At. Mol. Opt. Phys.* 22, 1307.
Robicheaux, F. (1993). *Phys. Rev. A.* 47, 1391.
Robicheaux, F., and Shaw, J. (1996). Submitted to *Phys. Rev. Lett.*
Rottke, H., and Welge, K. H. (1986). *Phys. Rev. A.* 33, 301.
Sandner, W. (1987). *Comm. At. Mol. Phys.* 20, 171.
Stapelfeldt, H., Papaioannou, D. G., Noordam, L. D., and Gallagher, T. F. (1991). *Phys. Rev. Lett.* 67, 3223.
Story, J. G., Duncan, D. I., and Gallagher, T. F. (1993a). *Phys. Rev. Lett.* 71, 3431.
Story, J. G., Duncan, D. I., and Gallagher, T. F. (1993b). *Phys. Rev. Lett.* 70, 3012.
Tielking, N. E., Bensky, T. J., and Jones, R. R. (1995). *Phys. Rev. A.* 51, 3370.
van de Water, W., Mariani, D. R., and Koch, P. M. (1984). *Phys. Rev. A.* 30, 2399.
van Druten, N. J., and Muller, H. G. (1995). *Phys. Rev. A.* 52, 3047.
van Druten, N. J., and Muller, H. G. (1996). *J. Phys. B: At. Mol. Opt. Phys.* 29, 15.
van Druten, N. J., Constantinescu, R. C., Schins, J. M., Nieuwenhuize, H., and Muller, H. G. (1997). *Phys. Rev. A.* 55, 622.
van Leeuwen, K. A. H., Oppen, G. V., Renwick, S., Bowlin, J. B., Koch, P. M., Jensen, R. V., Rath, O., Richards, D., and Leopold, J. G. (1985). *Phys. Rev. Lett.* 55, 2231.
Vos, R. J., and Gavrila, M. (1993). *Phys. Rev. A.* 48, 46.
Vrijen, R. B., Hoogenraad, J. H., Muller, H. G., and Noordam, L. D. (1993). *Phys. Rev. Lett.* 70, 3016.
Vrijen, R. B., Hoogenraad, J. H., and Noordam, L. D. (1994). *Modern Physics Letters B.* 8, 205.
Vrijen, R. B., and Noordam, L. D. (1996). *J. Opt. Soc. Am. B.* 13, 189.
Vrijen, R. B., van Ingen, M., and Noordam, L. D. in H. G. Muller and M. V. Fedorov (Eds.), *Super-Intense Laser-Atom Physics IV.* Kluwer Academic Publishers (Dordrecht/Boston/London, 1996), pp. 23–35.
Vrijen, R. B. (1997). Ph.D. thesis, University of Amsterdam. (The Netherlands).
Wang, X., and Cooke, W. E. (1991). *Phys. Rev. Lett.* 67, 976.
Wang, X., and Cooke, W. E. (1992). *Phys. Rev. A.* 46, 4347.
Watkins, R. B., Vrijen, R. B., Griffith, W. M., and Gallagher, T. F. (1996). Submitted to *Phys. Rev. A.*
Yeazell, J. A., and Stroud Jr., C. R. (1991). *Phys. Rev. A.* 43, 5153.
You, D., Jones, R. R., Bucksbaum, P. H., and Dykaar, D. R. (1993). *Opt. Lett.* 18, 290.